SustainGym: Reinforcement Learning Environments for Sustainable Energy Systems

Christopher Yeh[1], **Victor Li**[1], **Rajeev Datta**[1], **Julio Arroyo**[1], **Nicolas Christianson**[1], **Chi Zhang**[2], **Yize Chen**[3], **Mehdi Hosseini**[4], **Azarang Golmohammadi**[4], **Yuanyuan Shi**[2], **Yisong Yue**[1], **Adam Wierman**[1]

[1]California Institute of Technology
[2]University of California, San Diego
[3]Hong Kong University of Science and Technology
[4]Beyond Limits
[1]{cyeh,vhli,rdatta,jarroyoi,yyue,adamw}@caltech.edu
[2]chz056@ucsd.edu, yyshi@eng.ucsd.edu
[3]yizechen@ust.hk
[4]{mhosseini, agolmohammadi}@beyond.ai

Abstract

The lack of standardized benchmarks for reinforcement learning (RL) in sustainability applications has made it difficult to both track progress on specific domains and identify bottlenecks for researchers to focus their efforts. In this paper, we present SustainGym, a suite of five environments designed to test the performance of RL algorithms on realistic sustainable energy system tasks, ranging from electric vehicle charging to carbon-aware data center job scheduling. The environments test RL algorithms under realistic distribution shifts as well as in multi-agent settings. We show that standard off-the-shelf RL algorithms leave significant room for improving performance and highlight the challenges ahead for introducing RL to real-world sustainability tasks.

1 Introduction

While reinforcement learning (RL) algorithms have demonstrated tremendous success in applications ranging from game-playing, *e.g.*, Atari and Go, to robotic control, *e.g.*, [1–3], most RL algorithms continue to only be benchmarked using toy environments—*e.g.*, OpenAI Gym [4]. These toy environments generally do not have realistic physical constraints, nor realistic environmental shifts over time. Furthermore, these environments are generally limited to single-agent systems, whereas real-world systems tend to involve coordination and/or competition between actors. The realism gap limits the reliable deployment of off-the-shelf RL algorithms in real-world systems.

Developing better RL algorithms to address these challenges requires a means of empirically benchmarking and comparing the performance of different algorithms in real-world settings. Our inspiration comes from progress in supervised machine learning (ML), where widespread adoption of breakthrough techniques was fueled by large datasets with standardized benchmarks, such as ImageNet for computer vision [5] and the GLUE benchmark for natural language processing [6]. More recently, many supervised learning datasets have been created to address specific real-world sustainability challenges, such as monitoring global progress towards sustainable development goals [7].

In this work, we introduce SustainGym, a suite of 5 RL environments that realistically model sustainability settings, summarized in Table 1:

Table 1: Summary of environments included in SustainGym and their features. The "Single agent" and "Multi-agent" rows indicate what an individual RL agent controls in that environment.

Env	EVChargingEnv	ElectricityMarketEnv	DatacenterEnv	CogenEnv	BuildingEnv
Control task	charging rates for EV charging stations	market bids for a grid-connected battery storage system	virtual capacity curve for a carbon-aware data center	dispatch set points for turbines	heating supply for buildings
Modeled after	charging networks at Caltech & JPL	generic test case (IEEE RTS-GMLC)	(loosely) a Google data center	specific combined cycle gas generation plant in the U.S.	generic DoE commercial reference building models
Single agent	all EV charging stations	single battery system	single data center	all 4 turbine units	all buildings
Multi-agent	one EV charging station, cooperative	N/A	N/A	one turbine unit, cooperative	one room, cooperative
Actions	discrete or continuous	discrete or continuous	continuous	mixed discrete & continuous	discrete or continuous
Rewards	cost + CO_2	cost + CO_2	penalty + CO_2	cost + CO_2	temperature difference + energy use
Distribution shift	MOER, EV arrivals	MOER, load	MOER	renewable wind penetration	outdoor temperature

- `EVChargingEnv` models the problem of scheduling electric vehicle (EV) charging to meet user needs while minimizing CO_2 emissions.
- `ElectricityMarketEnv` models a grid-scale battery storage system bidding into the electricity market to generate profit (through price arbitrage) and reduce CO_2 emissions.
- `DatacenterEnv` models a datacenter deciding on a "virtual capacity curve" to shift flexible jobs towards times of day with lower CO_2 emissions.
- `CogenEnv` models a combined cycle cogeneration plant producing steam and electricity to meet local demand while minimizing fuel usage and ramp costs.
- `BuildingEnv` models the thermal control of building energy systems to reduce the total electricity consumption while satisfying the user-specified temperature requirement.

A key feature of SustainGym environments is their support for testing RL algorithms under realistic and natural exogenous distribution shifts, which generally fall under two categories:

1. *Shifts in demand.* In each environment, RL agents choose actions to satisfy some "demand" that is often affected by the behavior of unmodeled agents. For example, in `EVChargingEnv`, the demand is the amount of energy that needs to be delivered to EVs that have arrived at the charging network. This demand changed significantly at the start of the COVID-19 pandemic when EV drivers changed their driving behaviors (Figure 2).
2. *Shifts in environmental parameters.* Real-world environments are rarely static, and SustainGym environments reflect changing environment parameters due to temporal and/or climate changes. For example, a battery storage controller for `ElectricityMarketEnv` makes decisions to minimize marginal CO_2 emissions, but the distribution of CO_2 emissions varies over time as power plants are added to or removed from the electric grid (Figure 1).

Notably, the distribution shifts reflected in SustainGym are unlike the "sim-to-real" or offline-vs-online RL distribution shifts that have been more commonly studied in the literature. The sim-to-real distribution shift comes from imperfect modeling of the environment, whereas the offline-to-online RL distribution shift is caused by a change in the policy used to generate trajectories. In contrast, the exogenous distribution shifts in SustainGym are not due to imperfect environments nor policy mismatches, but rather more fundamental changes in the transition dynamics of the Markov decision processes. Note that only the transition dynamics experience distribution shift; the state space, action space, and reward functions do not change.

Two other similar lines of work to the distribution shifts in SustainGym are nonstationary RL environments [8] and distributionally robust RL [9]. However, whereas nonstationary RL typically

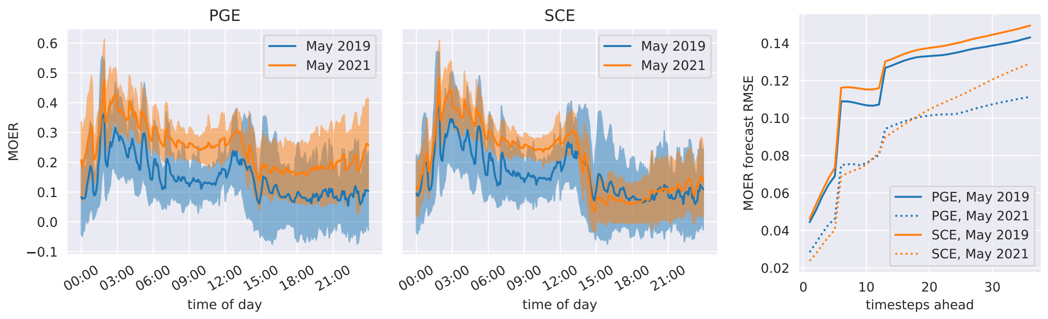

Figure 1: (left) MOER values from two different regions (a.k.a. "balancing authorities") in California, Pacific Gas & Electric (PGE) and Southern California Edison (SCE). Solid line is the mean MOER over all days in a month at a given time of day. Shaded region is ± 1 std. dev. (right) MOER forecast error increases with the forecast horizon.

evaluates an RL agent's performance over the course of a changing environment, SustainGym benchmarks RL agents' ability to generalize to new (unseen) distribution shifts. Distributionally robust RL generally assumes that the set of environmental distributions are known at training time, which is not necessarily the case for the settings considered in SustainGym.

In addition to modeling realistic distribution shifts, SustainGym is distinctive for its inclusion multi-agent interactions, physical constraints, and mixtures of discrete and continuous actions, as summarized in Table 1.

To demonstrate the use of the SustainGym, we perform experiments with off-the-shelf RL algorithms. We find that these algorithms have mixed performance on SustainGym. Furthermore, we show that distribution shifts may reduce the performance of these algorithms significantly, demonstrating a need for more robust algorithms. Finally, comparisons against non-RL baselines and oracles show that RL has significant room for improvement.

Due to page constraints, the main text of this paper summarizes key design choices and experimental observations for SustainGym. Details can be found in Appendix B. Code, licenses, and instructions for using SustainGym can be found on GitHub.[1]

Related Work. Prior work related to SustainGym includes ConservationGym, which focuses on ecological applications [10], PowerGridWorld for power system modeling and simulation [11], and CityLearn for simulation of demand response and urban energy management [12], among others. RL environments and algorithms for both EV charging [13–15] and electricity markets [16–18] have also been released. Compared to these works, the unique aspects of SustainGym are its focus on tracking estimated CO_2 emissions and its ability to test RL algorithms in settings with challenging distribution shifts, physical constraints, and interactions between multiple agents. We expect SustainGym to serve as a benchmark for the progress of RL algorithm development for sustainable energy systems.

2 Environments

This section introduces the 5 environments in SustainGym and summarizes their design choices.

Marginal CO_2 emissions. Three environments (`EVChargingEnv`, `ElectricityMarketEnv`, `DatacenterEnv`) impose a cost P_{CO_2} (in \$/kgCO_2) on the simulated CO_2 emissions induced by the actions of an agent as a result of changes in electricity consumption. To do so, our environments use data on California's historical marginal operating emissions rate (MOER, in kgCO_2/kWh), which is the increase in CO_2 emissions per increase in energy demand. The MOER at time t is denoted $m_t \in \mathbb{R}_+$, and the forecasts generated at time t for the next k time steps are denoted $\hat{m}_{t:t+k-1|t} \in \mathbb{R}^k$. By default, we use $k = 36$. Figure 1 shows how MOER values and their forecasts vary across time and between different regions in California.

[1]`https://github.com/chrisyeh96/sustaingym/`

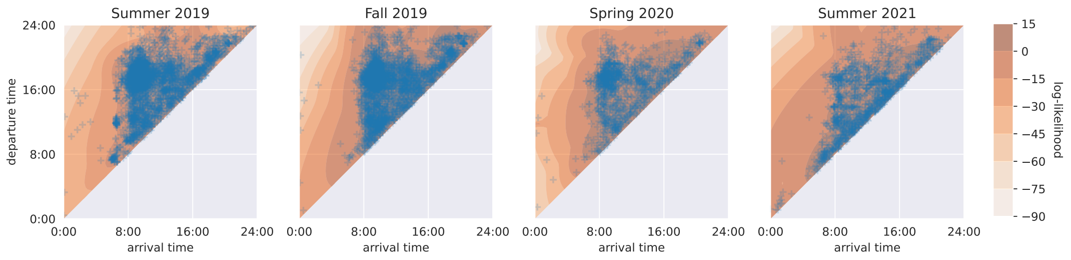

Figure 2: EV arrival vs. departure times for the Caltech EV charging network. Historical data is in blue, and log-likelihood contours from a 30-component GMM are in orange. The distribution of EV arrival and departure times changed noticeably when the COVID-19 pandemic began in early 2020.

2.1 `EVChargingEnv`

`EVChargingEnv` uses ACNSim [13] to simulate the charging of EVs based on actual data gathered from EV charging networks between fall 2018 and summer 2021 [19, 20]. ACNSim is a "digital twin" of actual EV charging networks at Caltech and JPL, which have $n = 54$ and 52 charging stations (abbrv. EVSEs, Electric Vehicle Supply Equipment), respectively. ACNSim accounts for nonlinear EV battery charging dynamics and unbalanced 3-phase AC power flows, and is thus very realistic. ACNSim (and therefore `EVChargingEnv`) can be extended to model other charging networks as well. When drivers charge their EVs, they provide an estimated time of departure and amount of energy requested. Because of network and power constraints, not all EVSEs can simultaneously provide their maximum charging rates (a.k.a. "pilot signals").

Each episode starts at midnight and runs at 5-minute time steps for 24 hours. At each time step, the agent simultaneously decides all n EVSE pilot signals to be executed for the duration of that time step. Its objective is to maximize charge delivery while minimizing carbon costs and obeying the network and power constraints.

Observation Space. An observation at time t is $s(t) = (t, d, e, m_{t-1}, \hat{m}_{t:t+k-1|t})$. $t \in [0, 1]$ is the fraction of day. $d \in \mathbb{Z}^n$ is estimated remaining duration of each EV (in # of time steps). $e \in \mathbb{R}^n_+$ is remaining energy demand of each EV (in kWh). If no EV is charging at EVSE i, then $d_i = 0$ and $e_i = 0$. If an EV charging at EVSE i has exceeded the user-specified estimated departure time, then d_i becomes negative, while e_i may still be nonzero.

Action Space. `EVChargingEnv` exposes a choice of discrete actions $a(t) \in \{0, 1, 2, 3, 4\}^n$, representing pilot signals scaled down by a factor of 8, or continuous actions $a(t) \in [0, 1]^n$ representing the pilot signal normalized by the maximum signal allowed M (in amps) for each EVSE. Physical infrastructure in a charging network constrains the set $\mathcal{A}_t$ of feasible actions at each time step t [20]. Furthermore, the EVSEs only support discrete pilot signals, so $\mathcal{A}_t$ is nonconvex. To satisfy these physical constraints, `EVChargingEnv` can project an agent's action $a(t)$ into the convex hull of $\mathcal{A}_t$ and round it to the nearest allowed pilot signal, resulting in final normalized pilot signals $\tilde{a}(t)$. ACNSim processes $\tilde{a}(t)$ and returns the actual charging rate $M\bar{a} \in \mathbb{R}^n_+$ (in amps) delivered at each EVSE, as well as the remaining demand $e_i(t + 1)$.

Reward Function. The reward function is a sum of three components: $r(t) = p(t) - c_V(t) - c_C(t)$. The profit term $p(t)$ aims to maximize energy delivered to the EVs. The constraint violation cost $c_V(t)$ penalizes network and power constraint violations. Finally, the CO_2 emissions cost $c_C(t)$, which is a function of the MOER m_t and charging action, aims to reduce emissions by encouraging the agent to charge EVs when the MOER is low.

Distribution Shift. `EVChargingEnv` supports real historical data as well as data sampled from a 30-component Gaussian Mixture Model (GMM) fit to historical data. We fitted GMMs to 4 disjoint historical periods, as defined in [21]. Figures 2 and 6 show the distribution of arrival and departure times in each of these 4 periods, for both the historical data as well as the GMM log-likelihoods. From these figures, it is evident that the pattern of user arrival and departure times changes over time, with the most drastic shift happening between Fall 2019 and Spring 2020, which is when the COVID-19 pandemic began.

Multiagent Setting. The multiagent setting features n agents, each deciding the pilot signal for a single EVSE. The reward is split evenly among the agents. Each agent obtains the global observation, except that the estimated remaining durations and energy demands for other EVSEs are delayed by t_d time steps.

2.2 `ElectricityMarketEnv`

`ElectricityMarketEnv` simulates a realtime electricity market for 33 generators and 1 80MWh battery storage system connected on a 24-bus congested transmission network based on the widely-used IEEE RTS-24 test case [22], with 5-minute settlements and load data from IEEE RTS-GMLC [23]. While `ElectricityMarketEnv` is not modeled after any particular real-world transmission network, the RTS-GMLC electricity load profile was designed to be representative of a modern transmission network located in the southwestern U.S.

All participants submit bids to the market operator (MO) at every time step. Based on the bids, the MO solves the multi-timestep security-constrained economic dispatch (SCED) problem which determines the price and amount of electricity purchased from (or sold by) each generator and battery to meet realtime electricity demand. Each episode runs for 1 day, with 5-minute time intervals. The agent controls the battery system and is rewarded for submitting bids that result in charging (buy) when prices are low, and discharging (sell) when prices and CO_2 emissions are high, thus performing price arbitrage.

Observation Space. An observation is $s(t) = (t, e, a(t-1), x_{t-1}, p_{t-1}, l_{t-1}, \hat{l}_{t:t+k-1}, m_{t-1}, \hat{m}_{t:t+k-1|t})$. $t \in [0, 1]$ represents the time of day. $e \in \mathbb{R}_+$ is the agent's battery level (in MWh). $a(t-1) \in \mathbb{R}_+^{2\times k}$ is the previous action taken. $x_{t-1} \in \mathbb{R}$ is the previous dispatch (in MWh) asked of the agent. $p_{t-1} \in \mathbb{R}_+$ is the previous price experienced by the agent (in \$/MWh). $l_{t-1} \in \mathbb{R}_+$ is the previous demand experienced by the agent (in MWh), while $\hat{l}_{t:t+k-1} \in \mathbb{R}^k$ is the forecasted demand for the next k steps.

Action Space. An agent action is a bid $a(t) = (a^c, a^d) \in \mathbb{R}_+^k \times \mathbb{R}_+^k$, representing prices (\$/MWh) that the agent is willing to pay (or receive) for charging (or discharging) per MWh of energy, for the next $k+1$ time steps starting from time t. The generators are assumed to always bid their fixed true cost of generation. The environment solves the optimal dispatch problem to determine the electricity price p_t and the agent's dispatch $x_t \in \mathbb{R}$, which is the amount of energy that the agent is obligated to sell into or buy from the grid within the next time step. The dispatch in turn determines the storage system's next energy level. We also provide a wrapper that discretizes the action space into 3 actions only: charge, do nothing, or discharge.

Reward Function. The reward function encourages the agent to maximize profit from charging decisions while minimizing associated carbon emissions. It is a sum of three components: $r(t) = r_R(t) + r_C(t) - c_T(t)$. The revenue term $r_R(t) = p_t x_t$ is the immediate revenue from the dispatch. The CO_2 emissions reward term $r_C(t) = P_{CO_2} m_t x_t$ represents the price of CO_2 emissions displaced or incurred by the battery dispatch. The terminal cost $c_T(t)$, which is nonzero only when $t = T$, encourages the battery to have the same energy level at the end of the day as when it started. We also provide an option to delay all reward signals until the terminal time (intermediate rewards are 0).

Distribution Shift. Distribution shift for `ElectricityMarketEnv` comes from changes in both electricity demand and MOER profiles between summer and winter months.

2.3 `DatacenterEnv`

`DatacenterEnv` is a simulator for carbon-aware job scheduling in datacenters, which aims to reduce the carbon emissions associated with electrcity usage in a datacenter. Carbon-aware job scheduling is premised upon two facts: (i) a significant fraction of a datacenter's workload (*e.g.*, up to 50% in some of Google datacenters [24, 25]) is comprised of low priority jobs whose execution can be delayed, and (ii) the carbon intensity of the electric grid fluctuates predictably over time. Therefore, if the execution of low priority workload is delayed to a time of day with "greener" energy, the datacenter's carbon emissions can be minimized.

`DatacenterEnv` is loosely modeled after a Google datacenter. We assume that jobs are scheduled according to a priority queue, with jobs spread evenly across the available machines. Following

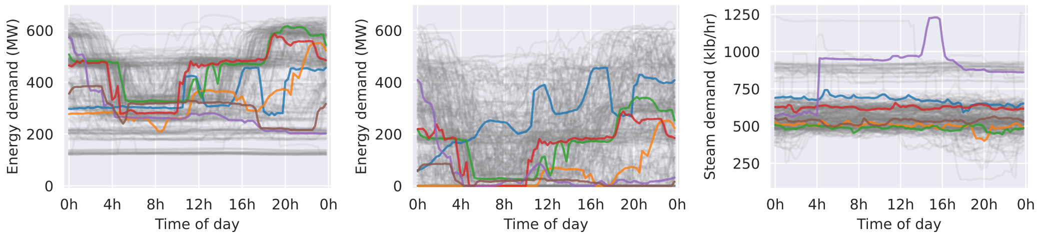

Figure 3: Electricity demand without (left) and with wind (middle), and steam demand (right) on a 15 minute basis for 253 days in `CogenEnv` dataset, with 6 random traces highlighted for each.

Radovanovic et al. [26], we implement workload execution delay by artificially limiting the total datacenter capacity with a *virtual capacity curve* (VCC) at each time step. If more jobs are enqueued than the VCC permits, then the jobs must wait until the VCC is raised high enough to allow the jobs to run. Simulation is carried out by replaying a sample of real job traces from a Google cluster from May 2019 [25]. One timestep in the environment corresponds to one hour, and each episode lasts the whole month.

Observation Space. An observation $s(t) = (a(t-1), d_t, n, \hat{m}_{t:t+23|t}) \in \mathbb{R}^{27}$ contains the active VCC $a(t-1)$ set from the previous time step, currently running compute load d_t, number of jobs waiting to be scheduled n, as well as the forecasted MOER for the next 24h $\hat{m}_{t:t+23|t}$.

Action Space. At time t, the agent sets the VCC, $a(t) \in [0, 1]$, for the next time step. This action denotes the *fraction* of the datacenter's maximum capacity allowed to be allocated by the scheduler.

Reward Function. The reward consists of two components that encourage the agents to trade-off between scheduling more jobs and reducing associated carbon emissions. The first component penalizes the agent when jobs are scheduled more than 24h after they were originally submitted. The second component is a carbon emissions cost. Formally, the reward is specified as

$$r(t) = d_t \cdot m_t + \mathbf{1}_{[t\%24=0]} \max\left(0, 0.97w_t - C\sum_{h=0}^{23} a(t-h)\right)$$

where $d_t \cdot m_t$ is the carbon emissions, C is the datacenter's maximum capacity, and w_t is the total job-hours of enqueued jobs on that day.

Distribution Shift. The distribution shift in `DatacenterEnv` comes from changes in the MOER between 2019 and 2021.

2.4 `CogenEnv`

`CogenEnv` simulates the operation of a combined cycle gas power plant tasked with meeting local steam and energy demand. Conventional dispatchable generators suffer decreased efficiency as a result of frequent ramping, posing a particular challenge as increasing penetrations of variable renewables necessitate larger and more frequent ramps to ensure supply-demand balance. Thus, optimal operation of cogeneration resources requires balancing the competing objectives of minimizing fuel use, anticipating future ramp needs, and ensuring delivery of sufficient energy and steam to the grid.

While `CogenEnv` models a specific combined cycle gas generation plant in the U.S. (anonymized and location withheld for security reasons), the basic environment setup is a representative prototype of more general dispatchable resource generation control tasks, due to its complexity (the number of variables, mixed continuous/binary decisions, complementary trains of the plant all needing to be controlled together). In addition, the environment is readily modifiable to accommodate other cost structures (*e.g.*, changing the relative magnitude of the constraint penalties vs. the ramping cost).

Observation Space. An observation takes the form

$$s(t) = (\tau, a(t-1), T_{t:t+k}, P_{t:t+k}, H_{t:t+k}, d^p_{t:t+k}, d^q_{t:t+k}, \pi^p_{t:t+k}, \pi^f_{t:t+k}),$$

where $\tau = t/96$ is the time (normalized by number of 15 minute intervals in a day), $a(t-1)$ is the agent's previous action, $T_{t:t+k}$, $P_{t:t+k}$, and $H_{t:t+k}$ are current and k forecast steps of temperature, pressure, and relative humidity, respectively, $d^p_{t:t+k}$ and $d^q_{t:t+k}$ are current and k forecast steps of electricity and steam demand, respectively, and $\pi^p_{t:t+k}$ and $\pi^f_{t:t+k}$ are current and k forecast steps of electricity and fuel price, respectively.

Action Space. The action space is a vector $a(t) \in \mathbb{R}^{15}$ specifying dispatch setpoints and other auxiliary variables for all turbines in the plant. Specifically, for each of three gas turbines, the agent specifies (a) a scalar turbine electricity output, (b) a scalar heat recovery steam flow, (c) a binary evaporative cooler switch setting, and (d) a binary power augmentation switch setting. In addition, for the steam turbine, the agent specifies (a) a scalar turbine electricity output, (b) a scalar steam flow through the plant condenser, and (c) an integer number of cooling tower bays employed.

Reward Function. The reward function is comprised of three components:

$$r(t) = -\left(r_f(a(t); T_t, P_t, H_t) + r_r(a(t); a(t-1)) + r_c(a(t); d^p_t, d^q_t)\right).$$

$r_f(a(t); T_t, P_t, H_t)$ is the generator fuel consumption in response to dispatch $a(t)$. $r_r(a(t); a(t-1))$ is the ramp cost, captured via an ℓ_1 norm penalty for any change in generator electricity dispatch between consecutive actions. $r_c(a(t); d^p_t, d^q_t)$ is a constraint violation penalty, penalizing any unmet electricity and steam demand, as well as any violation of the plant's dynamic operating constraints. The sum of these three components is negated to convert costs to rewards.

Distribution Shift. `CogenEnv` considers distribution shifts in the renewable generation profiles, and specifically, increasing penetration of wind energy. This increased variable renewable energy on the grid necessitates more frequent ramping in order to meet electricity demand, and may pose a challenge for RL algorithms trained on electricity demand traces without such variability.

Multiagent Setting. The multiagent setting treats each turbine unit (each of the three gas turbines and the steam turbine) as an individual agent whose action is the turbine's electricity dispatch decision and auxiliary variable settings. The negative reward of each agent is the sum of the corresponding turbine unit's fuel consumption, ramp cost, and dynamic operating constraint penalty, as well as a shared penalty for unmet electricity and steam demand that is split evenly across agents. All agents observe the global observation.

2.5 `BuildingEnv`

`BuildingEnv` considers the control of the heat flow in a multi-zone building so as to maintain a desired temperature setpoint. Building temperature simulation uses first-principled physics models. Users can either choose from a pre-defined list of buildings (Office small, School primary, Apartment midrise, and Office large) and three climate types and cities (San Diego, Tucson, New York) provided by the Department of Energy (DoE) Building Energy Codes Program [27] or define a customized `BuildingEnv` environment by importing any self-defined EnergyPlus building models. Each episode runs for 1 day, with 5-minute time intervals ($H = 288$, $\tau = 5/60$ hours).

Observation Space. For a building with M indoor zones, the state $s(t) \in \mathbb{R}^{M+4}$ contains observable properties of the building environment at timestep t:

$$s(t) = (T_1(t), \dots, T_M(t), T_{\mathrm{E}}(t), T_{\mathrm{G}}(t), Q^{\mathrm{GHI}}(t), \bar{Q}^{\mathrm{p}}(t)),$$

where $T_i(t)$ is zone i's temperature at time step t, $\bar{Q}^{\mathrm{p}}(t)$ is the heat acquisition from occupant's activities, $Q^{\mathrm{GHI}}(t)$ is the heat gain from the solar irradiance, and $T_{\mathrm{G}}(t)$ and $T_{\mathrm{E}}(t)$ denote the ground and outdoor environment temperature. In practice, the agent may have access to all or part of the state variables for decision-making depending on the sensor setup. Note that the outdoor/ground temperature, room occupancy, and heat gain from solar radiance are time-varying uncontrolled variables from the environment.

Action Space. The action $a(t) \in [-1, 1]^M$ sets the controlled heating supplied to each of the M zones, scaled to $[-1, 1]$.

Reward Function. The objective is to reduce energy consumption while keeping the temperature within a given comfort range. The default reward function is a weighted ℓ_2 reward, defined as

$$r(t) = -(1-\beta)\left\|a(t)\right\|_2 - \beta\|T^{\mathrm{target}}(t) - T(t)\|_2$$

where $T^{\mathrm{target}}(t) = [T^{\mathrm{target}}_1(t), \dots, T^{\mathrm{target}}_M(t)]^\top$ are the target temperatures and $T(t) = [T_1(t), \dots, T_M(t)]^\top$ are the actual zonal temperatures. `BuildingEnv` also allows users to customize reward functions by changing the weight term β or the parameter p defining the ℓ_p norm.

Table 2: Distribution shift experiments

Environment	What shifts	Original setting	Shifted setting
`EVChargingEnv`	EV sessions, MOER	Summer 2019	Summer 2021
`DatacenterEnv`	MOER	May 2019	May 2021
`CogenEnv`	Wind penetration	0 MW wind	300 MW wind
`BuildingEnv`	Ambient temperature	Summer 2004	Winter 2003

Users can customize the reward function to consider CO_2 emissions and temperature constraints such as upper and lower temperature bounds.

Distribution Shift. `BuildingEnv` features distribution shifts in the ambient outdoor temperature profile T_E which varies with different seasons. `BuildingEnv` supports the distribution shifts due to the variation of seasons, located cities of the buildings, and can examine the challenges brought by such shifts in the RL environment.

Multiagent Setting. In the multiagent setting for `BuildingEnv`, each agent controls the heating action for a single zone in the building. It must coordinate with other agents to maximize overall reward. Each agent obtains the same global observation and reward.

3 Experiments

For each of the 5 environments in SustainGym, we implemented baseline non-RL algorithms as well as off-the-shelf RL algorithms trained using either RLLib [28] or Stable-Baselines3 (SB3) [29]. For most environments, we tested off-policy soft actor-critic (SAC) [30] and on-policy proximal policy optimization (PPO) [31]. Note that neither RLLib nor SB3 has an implementation of SAC that supports mixed discrete and continuous actions, as found in `CogenEnv`. For `EVChargingEnv`, we also tested multi-agent implementations of PPO and SAC, where the same policy is shared across agents. Non-RL algorithms tested include random policies and model predictive control (MPC), which is a model-based controller. Detailed descriptions of the implementations for each algorithm, including hyper-parameter tuning, are given in Appendix B. Finally, to test distribution shift, we trained RL agents in both "original" and "shifted" environments, then compared their performance on the shifted environment, as described in Table 2.

4 Discussion and Conclusion

Our experiments, shown in Figure 4, demonstrate a wide range of outcomes for off-the-shelf RL algorithms, with no single algorithm outperforming all the rest. In `EVChargingEnv`, for example, most of the RL algorithms perform no better than random actions, with the exception of multi-agent PPO with discrete actions. On `DatacenterEnv` and `BuildingEnv`, we notice a wider spread of returns across the different RL algorithms. In contrast, model-based MPC algorithms, where available, tend to perform more consistently than most RL algorithms.

In terms of distribution shift, we see a wide range of outcomes between agents trained on the original environments versus the shifted environments. Surprisingly, in `CogenEnv`, both single-agent and multi-agent policies trained on the shifted environment perform worse on the shifted environment than agents trained on the original environment. We believe this result may be due to the increased variability of shifted environment, making the shifted environment harder to learn in. In `DatacenterEnv`, the shift in MOER values shows essentially no effect on agent performance. In `EVChargingEnv`, agents trained on the shifted environment generally perform slightly better than agents trained on the original environment. In `BuildingEnv`, agents trained on the shifted environment perform much better.

These results highlight that the distribution shifts present in SustainGym environments provide substantial opportunities for future research, including robust RL algorithms [32] as well as online learning under distribution shift. Developing RL algorithms that are robust to these natural distribution shifts will be critical for deploying RL in the real-world high-impact sustainability settings such as those modeled by SustainGym environments.

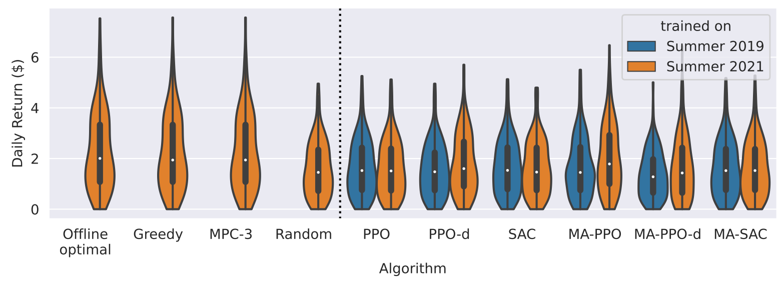

(a) `EVChargingEnv`

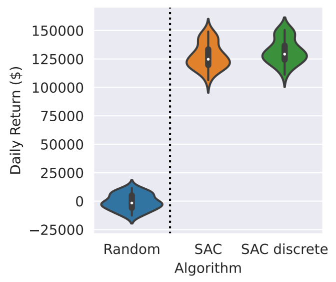

(b) `ElectricityMarketEnv`

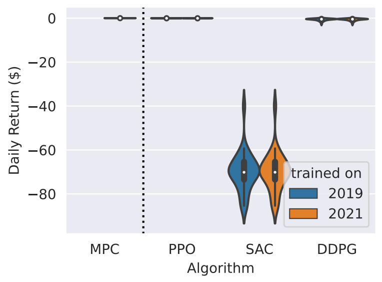

(c) `DatacenterEnv`

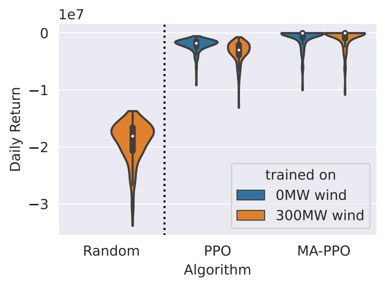

(d) `CogenEnv`

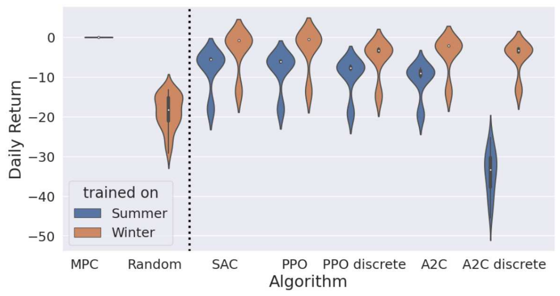

(e) `BuildingEnv`

Figure 4: Experimental results for all 5 environments comparing performance on the shifted environment between RL algorithms trained on the original environment (blue) and RL algorithms trained on the shifted environment (orange). Policies using discretized actions are indicated with "-d", and multi-agent policies are prefixed with "MA-". For a complete description of the experiments, please see Appendix B.

Multi-agent RL. SustainGym is currently designed to support multi-agent RL in 3 environments, with the goal of upgrading all environments with multi-agent support in the future. In the two environments for which we tested multi-agent RL policies (`EVChargingEnv` and `CogenEnv`), the multi-agent PPO (MA-PPO) policies out-performed all other RL policies. We suspect that this may be because the action spaces in these environments factorize well across agents, so the multi-agent policies can learn more efficiently. Furthermore, we suspect that multi-agent policies may have the potential of performing better under distribution shift, since their environments are naturally non-stationary during training. We notice this to be true for both `EVChargingEnv` and `CogenEnv`: of the RL policies trained on the original environments, the multi-agent policies performed best when tested on the shifted environment.

Future work. SustainGym is under active development, with several key directions of future work:

- Comprehensive support for multi-agent RL. Currently, only 3 out of the 5 environments support multi-agent RL. We are working to extend the two other environments `ElectricityMarketEnv` and `DatacenterEnv` to the multi-agent RL setting. For `ElectricityMarketEnv`, we plan on introducing multiple batteries into the same transmission network, each controlled by separate competing agents. This will be the first

competitive multi-agent RL environment in SustainGym. (All other environments feature cooperative multi-agent RL.) For `DatacenterEnv`, we plan on introducing multiple datacenters spread across geographic regions to enable both temporal and geographic carbon-aware load shifting. Each datacenter would be its own agent.
- Different degrees of distribution shift. Currently, SustainGym environments feature a binary choice of distribution shift: an original environment, and a shifted environment. We plan on introducing more settings with varying degrees of distribution shift.
- More environments. We welcome new environment ideas and contributions to SustainGym and are working with potential collaborators to extend the scope of environments.

Limitations We conclude by acknowledging general limitations of SustainGym. First, SustainGym only captures very limited dimensions of sustainability (*i.e.*, energy and CO_2 emissions) and does not account for other aspects such as water usage and other pollutants associated with energy production. We welcome collaboration with experts in these other sustainability domains to help us improve the sustainability mission of SustainGym. Second, SustainGym is limited in the types of distribution shifts that are considered. Finally, while SustainGym environments have been designed to be reasonably representative of various sustainable energy settings, there is inevitably a gap between SustainGym simulations and actual hardware systems. A detailed discussion of the representativeness, generalizability, and limitations of each environment can be found in Appendix B.

Acknowledgments and Disclosure of Funding

We would like to acknowledge Steven Low, Tongxin Li, Zachary Lee, Lucien Werner, Zaiwei Chen, Ivan Jimenez, Pieter Van Santvliet, and Ameera Abdelaziz for their feedback and input during the preparation of SustainGym. The model underlying `CogenEnv` was developed in partnership with Beyond Limits and Enexsa. Funding for this project comes from a variety of sources, including NSF awards CNS-2146814, CPS-2136197, CNS-2106403, EPCN-2200692, and NGSDI-2105648; an NSF Graduate Research Fellowship; an Amazon AI4Science Fellowship; the Resnick Sustainability Institute; Hellman Fellowship; Amazon Web Services; and Beyond Limits. This work is partially supported by the Department of the Air Force under Air Force Contract No. FA8702-15-D-0001. Any opinions, findings, conclusions or recommendations expressed in this material are those of the author(s) and do not necessarily reflect the views of the Department of the Air Force. Notwithstanding any copyright notice, U.S. Government rights in this work are defined by DFARS 252.227-7013 or DFARS 252.227-7014 as detailed above. Use of this work other than as specifically authorized by the U.S. Government may violate any copyrights that exist in this work.

References

[1] Volodymyr Mnih, Koray Kavukcuoglu, David Silver, Andrei A. Rusu, Joel Veness, Marc G. Bellemare, Alex Graves, Martin Riedmiller, Andreas K. Fidjeland, Georg Ostrovski, Stig Petersen, Charles Beattie, Amir Sadik, Ioannis Antonoglou, Helen King, Dharshan Kumaran, Daan Wierstra, Shane Legg, and Demis Hassabis. Human-level control through deep reinforcement learning. *Nature*, 518(7540):529–33, February 2015. ISSN 1476-4687. doi: 10.1038/nature14236. URL `https://www.nature.com/articles/nature14236`.

[2] David Silver, Julian Schrittwieser, Karen Simonyan, Ioannis Antonoglou, Aja Huang, Arthur Guez, Thomas Hubert, Lucas Baker, Matthew Lai, Adrian Bolton, Yutian Chen, Timothy Lillicrap, Fan Hui, Laurent Sifre, George van den Driessche, Thore Graepel, and Demis Hassabis. Mastering the game of Go without human knowledge. *Nature*, 550(7676):354–359, October 2017. ISSN 1476-4687. doi: 10.1038/nature24270. URL `https://www.nature.com/articles/nature24270`.

[3] Jens Kober, J. Andrew Bagnell, and Jan Peters. Reinforcement learning in robotics: A survey. *The International Journal of Robotics Research*, 32(11):1238–1274, September 2013. ISSN 0278-3649. doi: 10.1177/0278364913495721. URL `https://doi.org/10.1177/0278364913495721`.

[4] Greg Brockman, Vicki Cheung, Ludwig Pettersson, Jonas Schneider, John Schulman, Jie Tang, and Wojciech Zaremba. OpenAI Gym. *arXiv:1606.01540 [cs]*, June 2016. URL `http://arxiv.org/abs/1606.01540`.

[5] Olga Russakovsky, Jia Deng, Hao Su, Jonathan Krause, Sanjeev Satheesh, Sean Ma, Zhiheng Huang, Andrej Karpathy, Aditya Khosla, Michael Bernstein, Alexander C. Berg, and Li Fei-Fei. ImageNet Large Scale Visual Recognition Challenge. *International Journal of Computer Vision*, 115(3):211–252, December 2015. ISSN 1573-1405. doi: 10.1007/s11263-015-0816-y. URL `https://doi.org/10.1007/s11263-015-0816-y`.

[6] Alex Wang, Amanpreet Singh, Julian Michael, Felix Hill, Omer Levy, and Samuel R. Bowman. GLUE: A Multi-Task Benchmark and Analysis Platform for Natural Language Understanding. In *International Conference on Learning Representations*, September 2018. URL `https://openreview.net/forum?id=rJ4km2R5t7`.

[7] Christopher Yeh, Chenlin Meng, Sherrie Wang, Anne Driscoll, Erik Rozi, Patrick Liu, Jihyeon Lee, Marshall Burke, David B. Lobell, and Stefano Ermon. SustainBench: Benchmarks for Monitoring the Sustainable Development Goals with Machine Learning. In *Thirty-fifth Conference on Neural Information Processing Systems Datasets and Benchmarks Track (Round 2)*, 12 2021. doi: 10.48550/arXiv.2111.04724. URL `https://openreview.net/forum?id=5HR3vCylqD`.

[8] Sindhu Padakandla, Prabuchandran K. J, and Shalabh Bhatnagar. Reinforcement Learning in Non-Stationary Environments. *Applied Intelligence*, 50(11):3590–3606, November 2020. ISSN 0924-669X, 1573-7497. doi: 10.1007/s10489-020-01758-5. URL `http://arxiv.org/abs/1905.03970`.

[9] Elena Smirnova, Elvis Dohmatob, and Jérémie Mary. Distributionally Robust Reinforcement Learning, June 2019. URL `http://arxiv.org/abs/1902.08708`.

[10] Marcus Lapeyrolerie, Melissa S. Chapman, Kari E. A. Norman, and Carl Boettiger. Deep Reinforcement Learning for Conservation Decisions, June 2021. URL `http://arxiv.org/abs/2106.08272`.

[11] David Biagioni, Xiangyu Zhang, Dylan Wald, Deepthi Vaidhynathan, Rohit Chintala, Jennifer King, and Ahmed S. Zamzam. PowerGridworld: A Framework for Multi-Agent Reinforcement Learning in Power Systems. November 2021. doi: 10.48550/arXiv.2111.05969. URL `http://arxiv.org/abs/2111.05969`.

[12] Jose R. Vazquez-Canteli, Sourav Dey, Gregor Henze, and Zoltan Nagy. CityLearn: Standardizing Research in Multi-Agent Reinforcement Learning for Demand Response and Urban Energy Management, December 2020. URL `http://arxiv.org/abs/2012.10504`.

[13] Zachary J. Lee, Sunash Sharma, Daniel Johansson, and Steven H. Low. ACN-Sim: An Open-Source Simulator for Data-Driven Electric Vehicle Charging Research. *IEEE Transactions on Smart Grid*, 12(6):5113–5123, 11 2021. ISSN 1949-3061. doi: 10.1109/TSG.2021.3103156.

[14] Georgios Karatzinis, Christos Korkas, Michalis Terzopoulos, Christos Tsaknakis, Aliki Stefanopoulou, Iakovos Michailidis, and Elias Kosmatopoulos. Chargym: An EV Charging Station Model for Controller Benchmarking. IFIP Advances in Information and Communication Technology, pages 241–252, Cham, 2022. Springer International Publishing. ISBN 978-3-031-08341-9. doi: 10.1007/978-3-031-08341-9_20.

[15] Heba M. Abdullah, Adel Gastli, and Lazhar Ben-Brahim. Reinforcement Learning Based EV Charging Management Systems–A Review. *IEEE Access*, 9:41506–41531, 2021. ISSN 2169-3536. doi: 10.1109/ACCESS.2021.3064354.

[16] Hao Wang and Baosen Zhang. Energy Storage Arbitrage in Real-Time Markets via Reinforcement Learning. In *2018 IEEE Power Energy Society General Meeting (PESGM)*, pages 1–5, August 2018. doi: 10.1109/PESGM.2018.8586321.

[17] Hanchen Xu, Xiao Li, Xiangyu Zhang, and Junbo Zhang. Arbitrage of Energy Storage in Electricity Markets with Deep Reinforcement Learning, May 2019. URL `http://arxiv.org/abs/1904.12232`.

[18] Jun Cao, Dan Harrold, Zhong Fan, Thomas Morstyn, David Healey, and Kang Li. Deep Reinforcement Learning-Based Energy Storage Arbitrage With Accurate Lithium-Ion Battery Degradation Model. *IEEE Transactions on Smart Grid*, 11(5):4513–4521, September 2020. ISSN 1949-3061. doi: 10.1109/TSG.2020.2986333.

[19] Zachary J. Lee, Tongxin Li, and Steven H. Low. ACN-Data: Analysis and Applications of an Open EV Charging Dataset. In *Proceedings of the Tenth ACM International Conference on Future Energy Systems*, e-Energy '19, pages 139–149, New York, NY, USA, June 2019. Association for Computing Machinery. ISBN 978-1-4503-6671-7. doi: 10.1145/3307772.3328313. URL `https://doi.org/10.1145/3307772.3328313`.

[20] Zachary J. Lee, George Lee, Ted Lee, Cheng Jin, Rand Lee, Zhi Low, Daniel Chang, Christine Ortega, and Steven H. Low. Adaptive Charging Networks: A Framework for Smart Electric Vehicle Charging. *IEEE Transactions on Smart Grid*, 12(5):4339–4350, September 2021. ISSN 1949-3061. doi: 10.1109/TSG.2021.3074437. URL `https://ieeexplore.ieee.org/document/9409126`.

[21] Tongxin Li, Ruixiao Yang, Guannan Qu, Yiheng Lin, Steven Low, and Adam Wierman. Equipping Black-Box Policies with Model-Based Advice for Stable Nonlinear Control, June 2022. URL `http://arxiv.org/abs/2206.01341`.

[22] Probability Methods Subcommittee. Ieee reliability test system. *IEEE Transactions on Power Apparatus and Systems*, PAS-98(6):2047–2054, 1979. doi: 10.1109/TPAS.1979.319398.

[23] Clayton Barrows, Aaron Bloom, Ali Ehlen, Jussi Ikäheimo, Jennie Jorgenson, Dheepak Krishnamurthy, Jessica Lau, Brendan McBennett, Matthew O'Connell, Eugene Preston, Andrea Staid, Gord Stephen, and Jean-Paul Watson. The IEEE Reliability Test System: A Proposed 2019 Update. *IEEE Transactions on Power Systems*, 35(1):119–127, January 2020. ISSN 1558-0679. doi: 10.1109/TPWRS.2019.2925557.

[24] Abhishek Verma, Luis Pedrosa, Madhukar R. Korupolu, David Oppenheimer, Eric Tune, and John Wilkes. Large-scale cluster management at Google with Borg. In *Proceedings of the European Conference on Computer Systems (EuroSys)*, Bordeaux, France, 2015. URL `https://research.google/pubs/pub43438/`.

[25] Muhammad Tirmazi, Adam Barker, Nan Deng, Md Ehtesam Haque, Zhijing Gene Qin, Steven Hand, Mor Harchol-Balter, and John Wilkes. Borg: the Next Generation. In *EuroSys'20*, Heraklion, Crete, 2020. URL `https://research.google/pubs/pub49065/`.

[26] Ana Radovanovic, Ross Koningstein, Ian Schneider, Bokan Chen, Alexandre Duarte, Binz Roy, Diyue Xiao, Maya Haridasan, Patrick Hung, Nick Care, et al. Carbon-aware computing for datacenters. *IEEE Transactions on Power Systems*, 38(2):1270–1280, 2022.

[27] The Building Energy Codes Program. Prototype building models. URL `https://www.energycodes.gov/prototype-building-models`.

[28] Eric Liang, Richard Liaw, Robert Nishihara, Philipp Moritz, Roy Fox, Ken Goldberg, Joseph Gonzalez, Michael Jordan, and Ion Stoica. Rllib: Abstractions for distributed reinforcement learning. In *International Conference on Machine Learning*, pages 3053–3062. PMLR, 2018.

[29] Antonin Raffin, Ashley Hill, Adam Gleave, Anssi Kanervisto, Maximilian Ernestus, and Noah Dormann. Stable-Baselines3: Reliable Reinforcement Learning Implementations. *Journal of Machine Learning Research*, 22(268):1–8, 2021. ISSN 1533-7928. URL `http://jmlr.org/papers/v22/20-1364.html`.

[30] Tuomas Haarnoja, Aurick Zhou, Pieter Abbeel, and Sergey Levine. Soft Actor-Critic: Off-Policy Maximum Entropy Deep Reinforcement Learning with a Stochastic Actor, August 2018. URL `http://arxiv.org/abs/1801.01290`.

[31] John Schulman, Filip Wolski, Prafulla Dhariwal, Alec Radford, and Oleg Klimov. Proximal Policy Optimization Algorithms, August 2017. URL `http://arxiv.org/abs/1707.06347`.

[32] Kishan Panaganti, Zaiyan Xu, Dileep Kalathil, and Mohammad Ghavamzadeh. Robust reinforcement learning using offline data. In S. Koyejo, S. Mohamed, A. Agarwal, D. Belgrave, K. Cho, and A. Oh, editors, *Advances in Neural Information Processing Systems*, volume 35, pages 32211–32224. Curran Associates, Inc., 2022. URL `https://proceedings.neurips.cc/paper_files/paper/2022/file/d01bda31bbcd780774ff15b534e03c40-Paper-Conference.pdf`.

[33] Timothy P. Lillicrap, Jonathan J. Hunt, Alexander Pritzel, Nicolas Heess, Tom Erez, Yuval Tassa, David Silver, and Daan Wierstra. Continuous control with deep reinforcement learning, July 2019. URL `http://arxiv.org/abs/1509.02971`.

[34] Aled James and Daniel Schien. A low carbon kubernetes scheduler. In *6th International Conference on ICT for Sustainability, ICT4S 2019*, volume 2382 of *CEUR Workshop Proceedings*. CEUR-WS, June 2019.

[35] Nicolas Christianson, Christopher Yeh, Tongxin Li, Mahdi Torabi Rad, Azarang Golmohammadi, and Adam Wierman. Robustifying machine-learned algorithms for efficient grid operation. In *NeurIPS 2022 Workshop on Tackling Climate Change with Machine Learning*, 2022. URL `https://www.climatechange.ai/papers/neurips2022/19`.

[36] J. King, A. Clifton, and B. Hodge. Validation of Power Output for the WIND Toolkit. Technical Report NREL/TP-5D00-61714, 1159354, September 2014. URL `http://www.osti.gov/servlets/purl/1159354/`.

[37] CAISO. What the duck curve tells us about managing a green grid. Technical report, California Independent System Operator, November 2016.

[38] Chi Zhang, Yuanyuan Shi, and Yize Chen. BEAR: Physics-Principled Building Environment for Control and Reinforcement Learning. In *Proceedings of the Fourteenth ACM International Conference on Future Energy Systems*, e-Energy '23. arXiv, November 2022. doi: 10.48550/arXiv.2211.14744. URL `http://arxiv.org/abs/2211.14744`.

[39] US DOE. Engineering reference. `https://energyplus.net/assets/nrel_custom/pdfs/pdfs_v22.1.0/EngineeringReference.pdf`, 2022.

[40] Volodymyr Mnih, Adrià Puigdomènech Badia, Mehdi Mirza, Alex Graves, Timothy P. Lillicrap, Tim Harley, David Silver, and Koray Kavukcuoglu. Asynchronous Methods for Deep Reinforcement Learning, June 2016. URL `http://arxiv.org/abs/1602.01783`.